Theoretical Results on Orbital Capture

H. BRYSK* AND M. E. ROSE

Oak Ridge National Laboratory, Oak Ridge, Tennessee

I. INTRODUCTION

THAT the study of the continuous beta spectrum is especially useful in providing information concerning nuclear decay schemes and in particular is most helpful in the assignment of angular momentum and parity values is well known. That orbital capture has not been as useful in providing such information is also well known. In the latter case, one can observe only the characteristic x-rays (or the Auger electrons), or the bremsstrahlung photon accompanying it. The first provides a measure of the appropriate decay constant. The second constitutes a useful method of measuring the maximum energy release,[1] thus supplementing the limited data of (p,n) thresholds.

Advances in experimental techniques in recent years have made reliable quantitative measurements of orbital capture possible, at the same time that the more accessible beta decays were being exhausted; consequently, there has been a sharp upsurge of interest in the field, some reflection of which can be gathered from two comparatively recent review articles.[2] The interpretation of the orbital capture data has been restricted by lack of readily available theoretical information. In an attempt to fill this need, the present authors issued a report[3] in which the theory was examined in detail, pertinent effects were treated explicitly, and the results of extensive numerical calculations were presented. The considerable interest expressed in this report indicates that a wider and more convenient dissemination of the results is desirable. In the present paper, the self-sufficiency of presentation striven for in the report has been given up, and previously published material is referred to rather than repeated. This paper contains the material which is original with us or not otherwise available in easily usable form, with some revisions (primarily through the incorporation of later numerical data) of the contents of the report referred to in the preceding.[3] Emphasis is on the final results and their use rather than on the details of calculation.

Section II consists of a discussion of transition probabilities and branching ratios. Transition probabilities are explicitly written down for the K shell and the L subshells for allowed through second-forbidden captures. While parts of this are available elsewhere, mostly implicitly, a full and consistent listing is undoubtedly much needed. This paper undertakes to supply this and to correct some errors in numerical factors in the published literature. The relative contributions of capture by the various subshells and of positron emission are examined in detail, with special attention to the hitherto neglected p electrons (L_{II} and L_{III} subshells) which can be very important in some circumstances. To give the reader a better qualitative grasp of the results, the discussion first uses approximate expressions from which trends can be more clearly exhibited in functional form, following these up with exact values where desirable. The figures supply the values of the bound electron radial wave functions (with corrections as described below) that appear in electron capture, and show the computed branching ratios in what we consider the most convenient form.

Section III outlines the procedure used in obtaining the electron wave functions. These are relativistic Coulomb radial functions corrected for the finite size of the nucleus and the effect of screening, and taking into account the variation in the electron wave function over the nuclear volume. Graphs of the corrections for finite-size and screening are given separately because they are of interest in other contexts.

II. TRANSITION PROBABILITIES AND BRANCHING RATIOS

A. Transition Probabilities

The formal treatment of orbital capture is similar to that of electron emission, with three differences:

(1) The electron wave functions correspond to bound states instead of particles in the continuum.

(2) For a given (sub) shell, the electron energy is discrete; it follows that the neutrino energy is also discrete.

(3) An electron in a given (sub) shell is in a definite total angular momentum state. There is no sum over angular momenta. The neutrino takes on all possible values of angular momentum consistent with the fixed electron angular momentum and the rank of the beta-decay tensor operator, the latter in turn being limited by the angular momenta of the initial and final nuclear states.

To obtain the probability of orbital capture one can take over the expressions for electron emission[4,5] by

* Now at the Radiation Laboratory, University of Michigan, Ann Arbor, Michigan.

[1] P. Morrison and L. I. Schiff, Phys. Rev. **58**, 24 (1940); D. Maeder and P. Preiswerk, Phys. Rev. **84**, 595 (1951).

[2] J. K. Major and L. C. Biedenharn, Revs. Modern Phys. **26**, 321 (1954); B. L. Robinson and R. W. Fink, Revs. Modern Phys. **27**, 424 (1955).

[3] H. Brysk and M. E. Rose, Oak Ridge National Laboratory Report No. 1830 (unpublished).

[4] E. Greuling, Phys. Rev. **61**, 568 (1942).

[5] D. L. Pursey, Phil. Mag. **42**, 1193 (1951).

TABLE I. Formulas for orbital capture transition probabilities $S_n^{(|\Delta J|)}$, for an interaction consisting of scalar and tensor couplings.[a]

Allowed (no parity change):

$|\Delta J|=1$:

K or $L_{\rm I}$: $S_0^{(1)}=(4/3)nq^2\alpha_{TT}I_1(0,\boldsymbol{\sigma})g^2$

$J=0\to0$:

K or $L_{\rm I}$: $S_0^{(0)}(0\to0)=(1/\pi)nq^2\alpha_{SS}K_0g^2$

$\Delta J=0$ (not $0\to0$):

$S_0^{(0)}=S_0^{(1)}+S_0^{(0)}(0\to0)$

First-forbidden (yes):

$|\Delta J|=1$:

K or $L_{\rm I}$: $S_1^{(1)}=(1/3\pi)nq^2R^{-2}\alpha_{SS}K_1[f^2+(2/3)qRfg+(1/3)q^2R^2g^2]$
$+(4/3)nq^2\alpha_{TT}\{I_1(0,\boldsymbol{\sigma}\times\mathbf{p}/M)g^2$
$+(2/3)R^{-2}I_1(1,\boldsymbol{\sigma})[f^2-(2/3)qRfg+(1/6)q^2R^2g^2]$
$-2(2/3)^{\frac12}R^{-1}I_1(0,1;\boldsymbol{\sigma},\boldsymbol{\sigma}\times\mathbf{p}/M)g[f-(1/3)qRg]\}$
$-(8/3)nq^2\alpha_{ST}\{(2/3)^{\frac12}R^{-2}J_1(1,\boldsymbol{\sigma})f^2$
$-(4\pi)^{-\frac12}R^{-1}J_1(0,\boldsymbol{\sigma}\times\mathbf{p}/M)g[f+(1/3)qRg]\}$

$J=0\to0$:

K or $L_{\rm I}$: $S_1^{(0)}(0\to0)=(4/3)nq^2R^{-2}\alpha_{TT}I_0(1,\boldsymbol{\sigma})$
$\times[f^2+(2/3)qRfg+(1/9)q^2R^2g^2]$

$\Delta J=0$ (not $0\to0$):

$S_1^{(0)}=S_1^{(1)}+S_1^{(0)}(0\to0)$

First-forbidden unique ($|\Delta J|=2$, yes):

K or $L_{\rm I}$: $S_1^{(2)}=(4/27)nq^4\alpha_{TT}I_2(1,\boldsymbol{\sigma})g^2$

$L_{\rm III}$: $S_1^{(2)}=(4/3)nq^2R^{-2}\alpha_{TT}I_2(1,\boldsymbol{\sigma})g^2$

Second-forbidden ($|\Delta J|=2$, no):

K or $L_{\rm I}$: $S_2^{(2)}=(2/45\pi)nq^4R^{-2}\alpha_{SS}K_2[f^2+(2/5)qRfg+(1/10)q^2R^2g^2]$
$+(4/45)nq^4\alpha_{TT}\{R^{-2}I_2(2,\boldsymbol{\sigma})$
$\times[f^2-(2/5)qRfg+(1/15)q^2R^2g^2]$
$+(5/3)I_2(1,\boldsymbol{\sigma}\times\mathbf{p}/M)g^2$
$-2(5/3)^{\frac12}I_2(2,1;\boldsymbol{\sigma},\boldsymbol{\sigma}\times\mathbf{p}/M)R^{-1}g[f-(1/5)qRg]$
$+(2\pi)^{-\frac12}(8/45)nq^4\alpha_{ST}\{R^{-2}J_2(2,\boldsymbol{\sigma})f^2$
$-(5/3)^{\frac12}R^{-1}J_2(1,\boldsymbol{\sigma}\times\mathbf{p}/M)g[f+(1/5)qRg]\}$

$L_{\rm III}$: $S_2^{(2)}=(2/5\pi)nq^2R^{-4}\alpha_{SS}K_2[f^2+(2/3)qRfg+(2/9)q^2R^2g^2]$
$+(4/5)nq^2R^{-2}\alpha_{TT}\{R^{-2}I_2(2,\boldsymbol{\sigma})$
$\times[f^2-(2/3)qRfg+(1/9)q^2R^2g^2]$
$+(5/3)I_2(1,\boldsymbol{\sigma}\times\mathbf{p}/M)g^2$
$-2(5/3)^{\frac12}R^{-1}I_2(2,1;\boldsymbol{\sigma},\boldsymbol{\sigma}\times\mathbf{p}/M)g[f-(1/3)qRg]\}$
$+(2\pi)^{-\frac12}(8/5)nq^2R^{-2}\alpha_{ST}$
$\times\{R^{-2}J_2(2,\boldsymbol{\sigma})[f^2-(1/9)q^2R^2g^2]$
$-(5/3)^{\frac12}R^{-1}J_2(1,\boldsymbol{\sigma}\times\mathbf{p}/M)g[f+(1/3)qRg]\}$

Second-forbidden unique ($|\Delta J|=3$, no):

K or $L_{\rm I}$: $S_2^{(3)}=(1/675)nq^6\alpha_{TT}I_3(2,\boldsymbol{\sigma})g^2$

$L_{\rm III}$: $S_2^{(3)}=(2/45)nq^4R^{-2}\alpha_{TT}I_3(2,\boldsymbol{\sigma})g^2$

[a] For $L_{\rm II}$, use the "K or $L_{\rm I}$" expressions with the substitutions $f\to g$, $g\to-f$.

replacing the continuum electron wave functions by bound state wave functions and selecting out of the sum over electron angular momenta that term which corresponds to the angular momentum of the orbit in question.[6] For the total capture probability, the transition probabilities due to each of the atomic electrons are then added up. Some terms, for which the order of forbiddenness exceeds the spin change, have been omitted in the above references[4,5]; however, these can be obtained from two related articles,[7,8] (except for some Fierz interference terms).

More explicitly, the published shape correction factors are expressed in terms of the following bilinear combinations of the electron wave functions, f and g, (for full nomenclature, see below):

$$\left.\begin{matrix}L_{k-1}\\P_{k-1}\end{matrix}\right\}=(2p^2F_0)^{-1}R^{2-2k}(g_{-k}^2\pm f_k^2),\tag{1a}$$

$$\left.\begin{matrix}M_{k-1}\\Q_{k-1}\end{matrix}\right\}=(2p^2F_0)^{-1}R^{-2k}(g_k^2\pm f_{-k}^2),\tag{1b}$$

$$\left.\begin{matrix}N_{k-1}\\R_{k-1}\end{matrix}\right\}=(2p^2F_0)^{-1}R^{1-2k}(f_{-k}g_{-k}\mp f_kg_k).\tag{1c}$$

The notation here differs from that of Greuling and Pursey in that we replace their $f_{-\kappa-1}$ by f_κ, and write $k=|\kappa|\geqslant1$. For reference, note that

$\kappa=-1$ for the K and $L_{\rm I}$ (sub) shells,

$\kappa=1$ for $L_{\rm II}$,

$\kappa=-2$ for $L_{\rm III}$.

For the corresponding electron capture expressions, replace $(2p^2F_0)^{-1}$ by $(\pi/2)q^2$ and then, for the K, $L_{\rm I}$, and $L_{\rm III}$ (sub) shells set $f_k=g_k=0$ in Eqs. (1), while for $L_{\rm II}$ set $f_{-k}=g_{-k}=0$ in Eqs. (1).

For electrons from the K shell and the three L subshells, the capture probabilities, S, are explicitly listed in Tables I and II for allowed through second-forbidden transitions. Terms of higher order with the same selection rules as the ones listed have been omitted, as have some of the same order which turn out to be numerically much smaller than the listed ones.

When we issued our report,[3] the weight of the experimental evidence was considered to point pretty conclusively to a beta-decay interaction consisting of tensor (T) and scalar (S) couplings only.[9] The transition probabilities for capture are listed in Table I for this choice of interaction. Recently, some of the evidence for this choice has been contradicted by other data, from which a mixture of axial vector (A) and vector (V) couplings emerges as favored. The transition probabilities for this latter choice are given in Table II. The advent of parity nonconservation in the theory has introduced a plenitude of coupling constants and consequent ambiguities that are not yet resolved. It is also giving rise to new types of experiments relevant to this question. Inclusion of all five types of coupling in one

[6] P. F. Zweifel, Phys. Rev. **96**, 1572 (1954); *ibid.* **107**, 329 (1957).

[7] E. J. Konopinski and G. E. Uhlenbeck, Phys. Rev. **60**, 308 (1941).

[8] A. M. Smith, Phys. Rev. **82**, 955 (1951).

[9] H. M. Mahmoud and E. J. Konopinski, Phys. Rev. **88**, 1266 (1952); H. Brysk, Phys. Rev. **94**, 1794 (1954).

table was avoided because of the resulting bulk and unwieldiness. If the beta-decay interaction turns out to contain more than two types of coupling (which seems improbable), it is doubtful that the measurements of lifetimes and branching ratios can be made to yield much useful information in the case of nonunique forbidden transitions because of the large number of interfering matrix elements involved.

In the so-called l-forbidden transitions, the chief contribution is usually (perhaps always) due to some admixture of an allowed transition, the result of deviation from a pure single-particle state, the more so the larger the comparative lifetime. The remaining, truly l forbidden, contribution includes all the second-forbidden terms listed in Tables I and II, additional second-forbidden terms which vanish for $|\Delta J|=2$, and also a small-component contribution of the matrix element of $(\beta)\boldsymbol{\sigma}$. Hence, to the extent that the l forbiddenness arises from pure single-particle states, there will be differences from the allowed behavior, particularly as to the extent of the contribution from the $L_{\rm III}$ shell. Conversely, an experimental investigation sufficiently precise to be able to detect these differences would reveal how pure the single-particle states really are.

The nomenclature used is as follows: the nuclear matrix element notation is that of Rose and Osborn,[10] except for the use of $(\mathbf{p}/M)$ rather than $\mathbf{p}$ as a variable. (Readers more accustomed to the Cartesian tensor notation will find the transcription in Tables I and II of reference 10.) For the coupling constants we use the abbreviation

$$\alpha_{XY}=C_X C_Y{}^*+C_X{}'C_Y{}'{}^*, \tag{2}$$

where C is the "parity-conserving" coupling constant and C' the "parity nonconserving" one. R is the nuclear radius which, in the usual relativistic units, we take as $0.426\alpha A^{\frac{1}{3}}$ (corresponding to $1.2\times10^{-13}A^{\frac{1}{3}}$ cm), where α is the fine structure constant and A the mass number. The relative occupancy of the X (sub) shell is denoted by n_X; i.e., $n_X=1$ if the parent atom has a filled X (sub) shell. The neutrino energy is $q_X=W_0+W_X$, where W_0 is the nuclear energy difference and W_X the energy of an X electron in mc^2 units, rest mass included. The Dirac radial functions are f and g. They have been used in the foregoing with subscripts denoting the quantum number κ. For convenience, the (sub) shell designation will be used alternatively as a subscript below. (The "large" components, the ones entering in the allowed and in the unique forbidden transitions, are g_K, $g_{L(\rm I)}$, $f_{L(\rm II)}$, and $g_{L(\rm III)}$; the "small" components are f_K, $f_{L(\rm I)}$, $g_{L(\rm II)}$, and $f_{L(\rm III)}$.)

Numerical values for the eight radial functions are given in Figs. 1–4 (for a detailed description of their computation see Sec. III). These values form the basis for all the quantitative results quoted below.

[10] M. E. Rose and R. K. Osborn, Phys. Rev. **93**, 1326 (1954).

TABLE II. Formulas for orbital capture transition probabilities $S_n^{(|\Delta J|)}$, for an interaction consisting of vector and axial vector couplings.[a]

Allowed (no parity change):

$|\Delta J|=1$:

K or $L_{\rm I}$: $S_0{}^{(1)}=(4/3)nq^2\alpha_{AA}I_1(0,\boldsymbol{\sigma})g^2$

$J=0\to0$:

K or $L_{\rm I}$: $S_0{}^{(0)}(0\to0)=(1/\pi)nq^2\alpha_{VV}K_0g^2$

$\Delta J=0$ (not $0\to0$):

$S_0{}^{(0)}=S_0{}^{(1)}+S_0{}^{(0)}(0\to0)$

First-forbidden (yes):

$|\Delta J|=1$:

K or $L_{\rm I}$: $S_1{}^{(1)}=(4/3)nq^2\alpha_{VV}\{I_1(0,\mathbf{p}/M)g^2$
$+(4\pi)^{-1}R^{-2}K_1[f^2-(2/3)qRfg+(1/3)q^2R^2g^2]$
$-i2(4\pi)^{-\frac{1}{2}}R^{-1}J_1(0,\mathbf{p}/M)g[f-(1/3)qRg]\}$
$+(8/9)nq^2R^{-2}\alpha_{AA}I_1(1,\boldsymbol{\sigma})$
$\times[f^2+(2/3)qRfg+(1/6)q^2R^2g^2]$
$-(8/3)nq^2\alpha_{VA}\{(2/3)^{\frac{1}{2}}R^{-2}J_1(1,\boldsymbol{\sigma})f^2$
$+i(2/3)^{\frac{1}{2}}R^{-1}I_1(0,1;\mathbf{p}/M,\boldsymbol{\sigma})g[f+(1/3)qRg]\}$

$J=0\to0$:

K or $L_{\rm I}$: $S_1{}^{(0)}(0\to0)=(1/\pi)nq^2\alpha_{AA}\{\mathcal{K}_0g^2+(4\pi/3)R^{-2}I_0(1,\boldsymbol{\sigma})$
$\times[f^2-(2/3)qRfg+(1/9)q^2R^2g^2]$
$-i2(4\pi/3)^{\frac{1}{2}}R^{-1}\mathcal{K}_0{}^{\frac{1}{2}*}T_{01}{}^0(r,\boldsymbol{\sigma})g[f-(1/3)qRg]\}$

$\Delta J=0$ (not $0\to0$):

$S_1{}^{(0)}=S_1{}^{(1)}+S_1{}^{(0)}(0\to0)$

First-forbidden unique ($|\Delta J|=2$, yes):

K or $L_{\rm I}$: $S_1{}^{(2)}=(4/27)nq^4\alpha_{AA}I_2(1,\boldsymbol{\sigma})g^2$

$L_{\rm III}$: $S_1{}^{(2)}=(4/3)nq^2R^{-2}\alpha_{AA}I_2(1,\boldsymbol{\sigma})g^2$

Second-forbidden ($|\Delta J|=2$, no):

K or $L_{\rm I}$: $S_2{}^{(2)}=(2/45\pi)nq^4\alpha_{VV}$
$\times\{R^{-2}K_2[f^2-(2/5)qRfg+(1/10)q^2R^2g^2]$
$+(10\pi/3)I_2(1,\mathbf{p}/M)g^2$
$-i2(10\pi/3)^{\frac{1}{2}}R^{-1}J_2(1,\mathbf{p}/M)g[f-(1/5)qRg]\}$
$+(4/45)nq^4R^{-2}\alpha_{AA}I_2(2,\boldsymbol{\sigma})$
$\times[f^2+(2/5)qRfg+(1/15)q^2R^2g^2]$
$+(2\pi)^{-\frac{1}{2}}(8/45)nq^4\alpha_{VA}\{R^{-2}J_2(2,\boldsymbol{\sigma})f^2$
$+i(10\pi/3)^{\frac{1}{2}}R^{-1}I_2(2,1;\boldsymbol{\sigma},\mathbf{p}/M)g[f+(1/5)qRg]\}$

$L_{\rm III}$: $S_2{}^{(2)}=(2/5\pi)nq^2R^{-2}\alpha_{VV}$
$\times\{R^{-2}K_2[f^2-(2/3)qRfg+(2/9)q^2R^2g^2]$
$+(10\pi/3)I_2(1,\mathbf{p}/M)g^2$
$-i2(10\pi/3)^{\frac{1}{2}}R^{-1}J_2(1,\mathbf{p}/M)g[f-(1/3)qRg]\}$
$+(4/5)nq^2R^{-4}\alpha_{AA}I_2(2,\boldsymbol{\sigma})$
$\times[f^2+(2/3)qRfg+(1/9)q^2R^2g^2]$
$+(2\pi)^{-\frac{1}{2}}(8/5)nq^2R^{-2}\alpha_{VA}$
$\times\{R^{-2}J_2(2,\boldsymbol{\sigma})[f^2-(1/9)q^2R^2g^2]$
$+i(10\pi/3)^{\frac{1}{2}}R^{-1}I_2(2,1;\boldsymbol{\sigma},\mathbf{p}/M)g[f+(1/3)qRg]\}$

Second-forbidden unique ($|\Delta J|=3$, no):

K or $L_{\rm I}$: $S_2{}^{(3)}=(1/675)nq^6\alpha_{AA}I_3(2,\boldsymbol{\sigma})g^2$

$L_{\rm III}$: $S_2{}^{(3)}=(2/45)nq^4R^{-2}\alpha_{AA}I_3(2,\boldsymbol{\sigma})g^2$

[a] For $L_{\rm II}$, use the "K or $L_{\rm I}$" expressions with the substitutions $f\to g$, $g\to-f$.

B. s Electrons

To make a semiquantitative comparison of corresponding subshells of different shells (i.e., states with the same angular momentum and parity but different principal quantum number n), we examine the non-

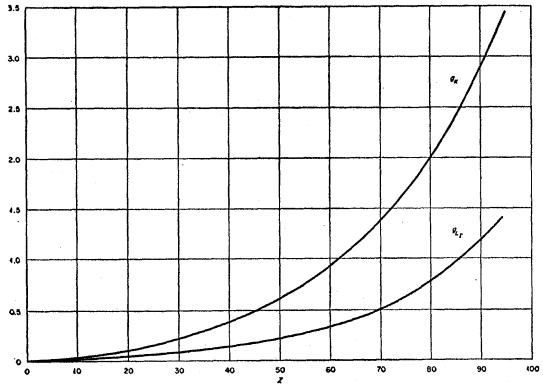

FIG. 1. Large radial wave functions for s electrons (g) evaluated at the nuclear radius.

relativistic radial wave functions for a hydrogen-like atom.[11] For small values of r (within the nucleus) and $l=0$, $g(r)\approx R_{n0}(r)\approx 2(\alpha Z/n)^{\frac{3}{2}}$ so that the transition probability falls off as n^{-3}. For $l\neq 0$, the n^{-3} dependence is still approximately satisfied. Relativistic wave functions have a modified behavior at the origin but, since this modified behavior is not influenced by the energy, the result holds for them too. Thus, the contributions from successive shells of states of a given angular momentum fall off, corresponding to the reduced probability density near the origin of states of higher n, but this decrease is not so steep that the higher n states can be neglected in the lifetime. Even where the energy available for the transition is far above the K-capture threshold, the L_{I} contribution is of the order of a tenth that of the K shell, and the higher shells may add as much as half of this correction. As the available energy approaches this threshold, the relative importance of the higher shells increases.

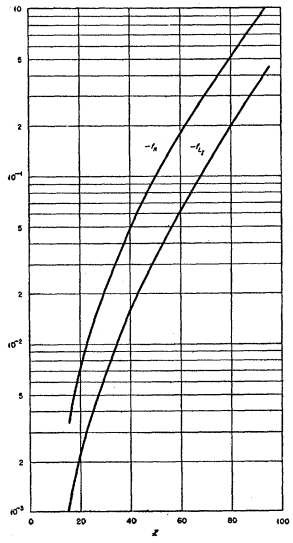

FIG. 2. Small radial wave functions for s electrons (f) evaluated at the nuclear radius. Note the logarithmic scale.

[11] H. Bethe, *Handbuch der Physik* (Springer-Verlag, Berlin, 1933), Vol. 24, p. 283.

The ratio $g_{L(\mathrm{I})}^2/g_K^2$ of screened relativistic Coulomb wave functions evaluated at the nuclear surface is given by Rose and Jackson.[12] The wave equations for the K shell and the L_{I} subshell differ only in the energy eigenvalue. Within the nucleus, the potential energy greatly exceeds the binding energy. After all corrections we find that $f_{L(\mathrm{I})}^2/f_K^2=g_{L(\mathrm{I})}^2/g_K^2$ within one percent. Provided that $q_K\approx q_{L(\mathrm{I})}$, i.e., that the energy available for the transition is not near the threshold for K capture, the probabilities of K and L_{I} capture, for any order of forbiddenness, are bilinear combinations of f and g with identical coefficients (which depend only on nuclear parameters). Then the L_{I}/K ratio is independent of the order of forbiddenness and is simply $g_{L(\mathrm{I})}^2/g_K^2$ (Fig. 5). On the other hand, near the K-capture threshold the neutrino energies are quite different for the two shells, and the L_{I}/K ratio depends seriously on $q_{L(\mathrm{I})}/q_K$ and also on the ratio of nuclear matrix elements (if more

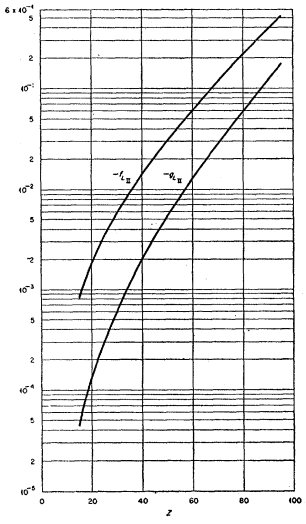

FIG. 3. The L_{II} radial wave functions evaluated at the nuclear radius. $f_{L(\mathrm{II})}$ is the large component, $g_{L(\mathrm{II})}$ is the small component. Note the logarithmic scale.

than one occurs). In fact, if the order of forbiddenness of the transition is known, it is then possible to obtain information as to the value of W_0 from the L_{I}/K ratio. Figure 6 demonstrates this for allowed transitions.

C. L_{II} Subshell

The L_{II} subshell differs from the L_{I} subshell in parity but has the same angular momentum. The change in parity reflects itself merely in a corresponding change in the parity of the neutrino wave function, so the selection rules for L_{II} are the same as for L_{I}, with the permutation of the radial functions $f\rightarrow g$, $g\rightarrow -f$. In the combinations $L_0\sim g_{-1}^2+f_1^2$, etc. that occur in beta-decay theory,[4,5] the first term contributes to the L_{I} subshell, the second term to the L_{II} subshell. For both subshells we have (in Bethe's notation[11]) $n=2\approx N$, $n'=1$; $\kappa=-1$ for L_{I}, $\kappa=+1$ for L_{II}. In the $r\rightarrow 0$ limit for low Z, we

[12] M. E. Rose and J. L. Jackson, Phys. Rev. **76**, 1540 (1949).

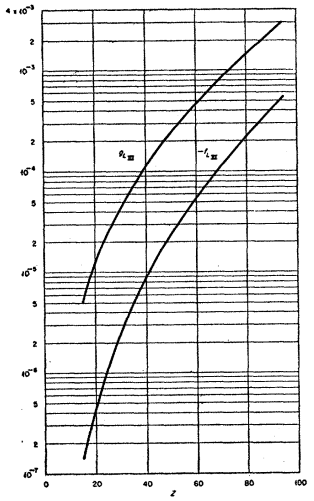

FIG. 4. The L_{III} radial wave functions evaluated at the nuclear radius. $g_{L(III)}$ is the large component; $f_{L(III)}$ is the small component. Note the logarithmic scale.

find from the expressions for the Coulomb radial functions[11] $f_{L(II)}^2/g_{L(I)}^2=3(1-W)/(1+W)\approx(3/16)\alpha^2Z^2$ so that the L_{II} wave functions (f,g) are consistently smaller (in magnitude) than the corresponding ones for L_I (g, f, respectively), the ratio never exceeding the order of ten percent and dropping off sharply for low Z. In comparing L_{II} with L_I capture, the difference in binding energy between the subshells can practically always be neglected. The ratio $f_{L(II)}^2/g_{L(I)}^2$ and $g_{L(II)}^2/f_{L(I)}^2$ differ from each other by about 10–30% (the lower figure applies to high Z where the ratio of L_{II}/L_I is largest—see Fig. 7). On the other hand, both ratios vary strongly with Z, changing by three orders of magnitude from $Z=15$ to $Z=95$. For allowed transitions or the unique type, the L_{II}/L_I capture ratio is $f_{L(II)}^2/g_{L(I)}^2$. For other transitions, the L_{II}/L_I ratio falls between $f_{L(II)}^2/g_{L(I)}^2$ and $g_{L(II)}^2/f_{L(I)}^2$; although the transcription leads from $(f_{L(I)}g_{L(I)})$ to $(-f_{L(II)}g_{L(II)})$ in the cross terms, $f_{L(I)}g_{L(I)}$ is negative while $f_{L(II)}g_{L(II)}$ is positive, so that the numerical values undergo no sign change. Hence, the L_{II}/L_I ratio is pretty much in-

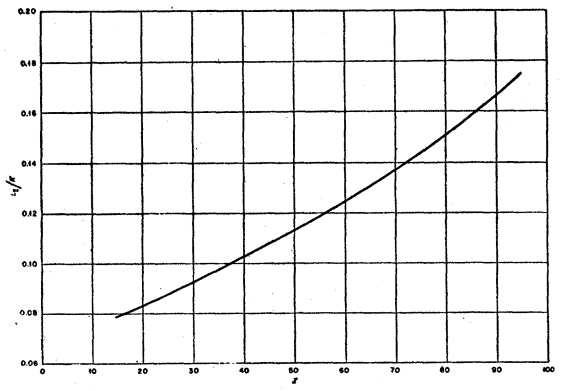

FIG. 5. $(g_{L(I)}/g_K)^2$ as a function of Z. This is the L_I/K branching ratio for all cases in which the energy release W_0 is large compared to the K-binding energy. In this case the function plotted applies to all orders of forbiddenness.

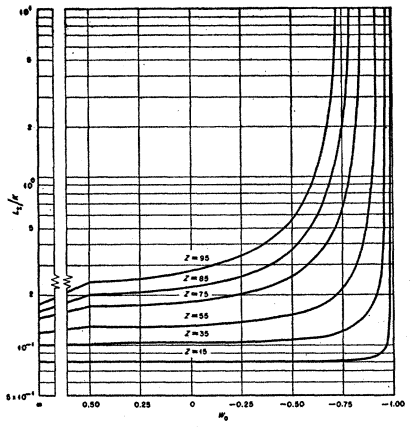

FIG. 6. $(g_{L(I)}q_{L(I)}/g_Kq_K)^2$ as a function of W_0 for various values of Z. This is the allowed L_I/K branching ratio and differs appreciably from the results in Fig. 5 only for W_0 near the K threshold.

sensitive to the order of forbiddenness, barring the rather negligible energy region where it is incorrect to assume $q_{L(II)}\approx q_{L(I)}$.

D. L_{III} Subshell

The L_{III} subshell has a different angular momentum than the other two L subshells ($\frac{3}{2}$ instead of $\frac{1}{2}$). This alters the selection rules. For allowed transitions, it forces the neutrino into a higher angular momentum state, resulting in the occurrence of an additional factor of the order of $(qR)^2$ in the transition probability. For first-forbidden ($|\Delta J|=0, 1$) transitions, the neutrino angular momentum can be the same as for the previous subshells. For $|\Delta J|\geq 2$, the neutrino may assume an angular momentum lower than for the previous subshells, so that now a factor of the order of $(qR)^{-2}$ enhances the L_{III} contribution. Comparing the L subshells in low Z approximation, we find that $-g_{L(III)}/f_{L(II)}\approx(2/3)R$ and $g_{L(III)}/g_{L(I)}\approx(1/2\cdot 3^{\frac{1}{2}})\alpha ZR$. Thus, the L_{III} subshell always makes a negligible contribution to allowed and first-forbidden ($|\Delta J|=0, 1$) transitions. For $|\Delta J|\geq 2$, on the other hand, the L_{III} subshell makes a contribution which is at least comparable to that of L_{II}, and which can in some circumstances become dominant.

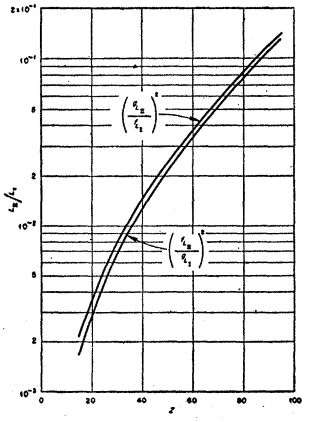

FIG. 7. $(f_{L(II)}/g_{L(I)})^2$ and $(g_{L(II)}/f_{L(I)})^2$ as functions of Z. The L_{II}/L_I branching ratio lies either on the first-named curve or between the two curves if the difference in L_I and L_{II} binding energies is neglected.

Looking at the matter more precisely, let us examine the first-forbidden unique transitions ($|\Delta J|=2$, yes). For an atom with a filled L shell, the capture ratio for the $L_{\rm III}$ and $L_{\rm I}$ subshells is

$$L_{\rm III}/L_{\rm I}=\frac{9g_{L(\rm III)}^2}{R^2g_{L(\rm I)}^2}\frac{(W_0+W_{L(\rm III)})^2}{(W_0+W_{L(\rm I)})^4}\approx\frac{9g_{L(\rm III)}^2}{q_L^2R^2g_{L(\rm I)}^2}, \quad (3)$$

where the last expression is obtained by neglecting the difference in binding energy between the subshells. It is clear that $L_{\rm III}$ capture is favored by small q_L, i.e., small W_0. To illustrate how the branching ratio behaves, let us select two particular values of W_0. First consider the energy to lie at the K-capture threshold, i.e., $W_0=-W_K$. Then $q_L=W_0+W_L=W_L-W_K\approx\frac{3}{8}\alpha^2Z^2$. Since $g_{L(\rm III)}^2/R^2g_{L(\rm I)}^2\approx\frac{1}{12}\alpha^2Z^2$, the $L_{\rm III}/L_{\rm I}$ ratio is now $16/3\alpha^2Z^2$. This is a large number; even for high Z (95 say), it is only down to 11. The exact $L_{\rm III}/L_{\rm I}$ ratio for $Z=95$ is 3 (a low Z approximation has its limitations for $Z=95$). On the other hand, if we raise the energy to the positron threshold ($W_0=1$), the importance of $L_{\rm III}$ diminishes. We now have $q_L\approx2$ and $L_{\rm III}/L_{\rm I}\approx(3/16)\alpha^2Z^2$. Even for $Z=95$, the exact $L_{\rm III}/L_{\rm I}$ ratio is now only 0.03 and $L_{\rm III}/K$ is less than 1%. The $L_{\rm III}/L_{\rm II}$ ratio is still nearly unity for $W_0=1$. It shows little Z dependence, varying from 1 for $Z=15$ to 0.2 for $Z=95$. Figure 8 exhibits the $L_{\rm III}/L_{\rm I}$ ratio for different Z's and W_0's. The sensitive energy dependence suggests using this branching ratio in first-forbidden unique transitions to determine W_0.

For second-forbidden ($|\Delta J|=2$) transitions, the $L_{\rm III}/L_{\rm I}$ ratio appears to be a bit larger, though the multiplicity of matrix elements precludes an exact statement. For second-forbidden unique transitions, the $L_{\rm III}/L_{\rm I}$ ratio is obtained from that quoted for first-forbidden unique by multiplication with a factor $(10/3)(q_{L(\rm III)}/q_{L(\rm I)})^2\approx10/3$.

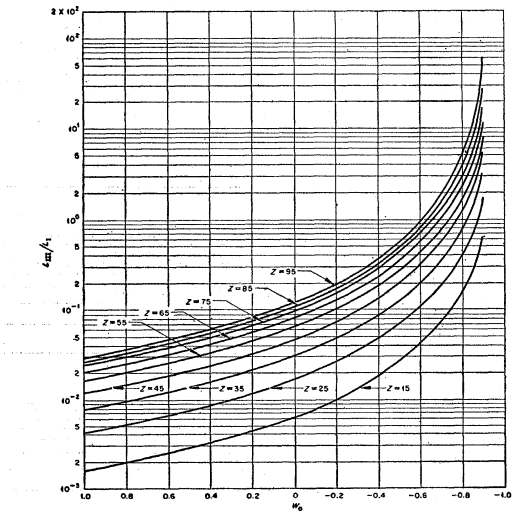

FIG. 8. The $L_{\rm III}/L_{\rm I}$ branching ratio for first-forbidden unique transitions as a function of W_0 for various values of Z. The binding energy difference between the L subshells has been included.

Thus we find that the $L_{\rm III}$ subshell makes a negligible contribution to $|\Delta J|=0, 1$ transitions. For $|\Delta J|=2$, its contribution is at least comparable to that of $L_{\rm II}$, increasing as the energy difference between the parent and product atoms decreases, and ultimately becoming dominant. For unique transitions the $L_{\rm III}/L_{\rm I}$ ratio could be used to deduce W_0 with due care not to apply the approximation $q_{L(\rm III)}\approx q_{L(\rm I)}$ when W_0 is so small that the difference in binding energy between the subshells is no longer negligible.

E. Capture-to-Positron Ratio

As we have seen, when positron emission is energetically possible capture occurs almost entirely from s-electron orbits, predominantly from the K shell. Graphs of the K/positron branching ratio for allowed transitions (calculated with Coulomb wave functions) have been given by Feenberg and Trigg[13]; Zweifel has computed values corrected for the effect of screening.[6] For orientation, let us disregard the small correction due to the p electrons and the energy difference between the K and L shells, and make the common approximations for the electronic wave functions that $\alpha Z\ll1$ and $\alpha Z/2R\gg1$. Then $f_{-1}\approx-(\alpha Z/2)g_{-1}$. To the beta-decay expressions[4] L_0, M_0, and N_0 there corresponds [see Eqs. (1)]

$$\begin{aligned}
&L_0\rightarrow(\pi/2)q^2(n_Kg_K^2+n_{L(\rm I)}g_{L(\rm I)}^2),\\
&M_0\rightarrow(\pi/2)q^2R^{-2}(n_Kf_K^2+n_{L(\rm I)}f_{L(\rm I)}^2)\\
&\qquad\approx(\pi/2)q^2(\alpha Z/2R)^2(n_Kg_K^2+n_{L(\rm I)}g_{L(\rm I)}^2), \quad (4)\\
&N_0\rightarrow-(\pi/2)q^2R^{-1}(n_Kf_Kg_K+n_{L(\rm I)}f_{L(\rm I)}g_{L(\rm I)})\\
&\qquad\approx-(\pi/2)q^2(\alpha Z/2R)(n_Kg_K^2+n_{L(\rm I)}g_{L(\rm I)}^2).
\end{aligned}$$

But, apart from the common factor $(\pi/2)q^2(n_Kg_K^2+n_{L(\rm I)}g_{L(\rm I)}^2)$, these are just the approximate values of these quantities for continuum electrons. The significance of this fact is as follows:

Allowed transitions involve L_0 only. First-forbidden transitions ($|\Delta J|=0, 1$) depend on a linear combination of L_0, M_0, and N_0 for the $S-T$ and $V-A$ interactions. Hence, to the approximation used above, the capture-to-positron ratio is about the same for allowed as for first-forbidden ($|\Delta J|=0, 1$) transitions, i.e., for all "allowed shape" transitions. The argument is weakened by the reversal of sign of the $S-T$ or $V-A$ cross term for capture as against positron emission, but this appears unlikely to upset the qualitative features. These statements cannot be refined because of our inaccurate knowledge of the relative magnitude of the matrix elements contributing to the first-forbidden nonunique transitions. For an interaction including other couplings the situation is further confused by the possible occurrence of energy-dependent interference terms (Fierz terms).

For first-forbidden ($|\Delta J|=2$) transitions, there is an

[13] E. Feenberg and G. Trigg, Revs. Modern Phys. **22**, 399 (1950).

energy dependent "correction factor" to the allowed shape spectrum. This correction factor is approximately proportional to p^2+q^2, whose mean value is roughly $(1/2)(W_0^2-1)$. The corresponding factor for capture is $q_K^2=(W_0+W_K)^2\approx(W_0+1)^2$. Hence, the capture-to-positron ratio is increased by a factor of about $2(W_0+1)/(W_0-1)$ as compared with the branching ratio for allowed transitions. This enhancement is traceable to the fact that there is about $2\,mc^2$ more energy available to capture than to positron emission. Since a single matrix element appears here, it is possible to improve the estimate by using the precise wave functions.

For higher forbidden transitions, the increase in the ratio is accentuated. For second-forbidden ($|\Delta J|=2$), there are shape correction factors proportional to (p^2+q^2), $(1/2)p^2+q^2$, and $(1/4)p^2+q^2$ associated with the various matrix elements, indicating some enhancement of the ratio, but the multiplicity of matrix elements prevents any precise statement. For second-forbidden ($|\Delta J|=3$), again a unique matrix element case, there is a factor compared with first-forbidden ($|\Delta J|=2$) of about the same magnitude as that linking the latter to allowed.

To sum up our investigation of the capture-to-positron ratio: The ratio apparently cannot tell whether an allowed shape transition is allowed or first-forbidden. It does show a detectable change for first-forbidden unique and higher forbidden transitions, intensified with increasing order of forbiddenness. However, these latter transitions can probably much more easily be identified on the basis of the shape of the positron spectrum and of the lifetime.

III. BOUND ELECTRON WAVE FUNCTIONS

In principle, to obtain the bound electron wave functions used in orbital capture, one should solve the Dirac equation for an electron in the field due to some sort of extended charge distribution (the nucleus) in the presence of other electrons (say, a Thomas-Fermi-Dirac calculation), and then perform some sort of weighted average over the nuclear volume. This would require a large scale machine computation, and have the additional disadvantage that to study the effect of a change of assumption at any point would require a complete rerun. Instead we start from the relativistic Coulomb wave functions[11] (a definite analytical form) and find the solution for a nucleus of finite size without screening (again an analytical form, though with approximations). We then obtain independently the effect of screening (in numerical form); this requires machine computation but fortunately we were able to extract it—as a bonus—from the printout of computations on internal conversion coefficients.[14] We treat analytically the average over the nuclear volume with the wave functions for the inside of a finite-size nucleus.

A. Finite Size of the Nucleus

The circumstance that the nuclear charge is distributed over a finite volume removes the singularity in the potential (at $r=0$) and also eliminates any singularity from the wave functions. To evaluate f and g at the nuclear surface, we make use of an identity satisfied by the Dirac radial functions for a central field,[15]

$$\frac{\partial}{\partial r}\left[r^2\left(f\frac{\partial g}{\partial W}-g\frac{\partial f}{\partial W}\right)\right]=r^2(f^2+g^2). \tag{5}$$

Upon integrating this equation, considering the integration space divided into two regions bounded by $r=R$ and matching the wave functions at the boundary, one obtains[15]

$$R^2g^2(R)=\left(\frac{\partial\rho_{\text{out}}}{\partial W}-\frac{\partial\rho_{\text{in}}}{\partial W}\right)^{-1}_{R,\,W'}, \tag{6}$$

where $\rho=f/g$ and ρ_{out} is the value of ρ obtained from solutions which are properly behaved at infinity while ρ_{in} is determined from solutions which are regular at the origin. Here W' is the energy eigenvalue, and *after* W' is inserted for W, $\rho_{\text{in}}\equiv\rho_{\text{out}}$. In every case the first term in the right hand side of (6) is positive, the second term negative. Equation (6) automatically yields normalized wave functions. In view of the smallness of the nuclear volume in comparison with the atomic volume, the former makes a negligible contribution to the normalization and the second term in the bracket can be ignored, as can be easily verified. Thus, except for an immaterial overall real phase factor, $f(R)$ and $g(R)$ can be evaluated in terms of the quantities ρ and $\partial\rho/\partial W$ (for the external solution) and the latter do not involve the normalization. The external wave functions differ from the point case in that the solution irregular at the origin is now admissible so that the wave function is a linear combination of two Whittaker functions.[16] The change in the potential results in a shift in the energy levels. While this shift is quite small, its inclusion is necessary to introduce the irregular solution. Since the charge distribution inside the nucleus is not known to an appreciable extent, the choice of potential in this region is rather arbitrary, except that it should remain finite at the origin, increase monotonically, and join continuously to the Coulomb potential outside the nucleus. Fortunately, the electronic wave functions are not overly sensitive to the choice of potential once these conditions are satisfied.[17] We used the simplest possible such potential which is, at the same time, a reasonable

[14] M. E. Rose *et al.* (unpublished). These computations were carried out on the National Bureau of Standards (Eastern) Automatic Computer—SEAC.

[15] M. E. Rose, Phys. Rev. **82**, 389 (1951).

[16] I. Malcolm and C. Strachan, Proc. Cambridge Phil. Soc. **47**, 610 (1951); I. Malcolm, Phil. Mag. **43**, 1011 (1952).

[17] M. E. Rose and D. K. Holmes, Phys. Rev. **83**, 190 (1951); Oak Ridge National Laboratory Report No. 1022 (unpublished).

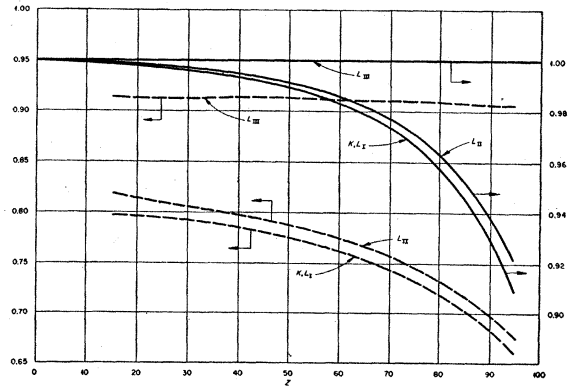

FIG. 9. Ratio of the radial wave functions at the nuclear radius for a finite size nucleus to the wave functions for a point nucleus. The full curves (right-hand ordinate scale) refer to the large components, the dashed curves (left-hand ordinate scale) to the small components.

one

$$V=-\frac{\alpha Z}{2R}\left(3-\frac{r^2}{R^2}\right), \tag{7}$$

which corresponds to a uniform nuclear charge distribution. The expression for the energy level shifts (from first-order perturbation) and the resulting ρ's and $\partial\rho/\partial W$'s are given in our report.[3] The leading term in the finite-size wave functions has the same R dependence as the Coulomb functions, so that the finite-size correction depends very little on the value chosen for the nuclear radius. The ratio of the finite-size wave function to the Coulomb wave function is given in Fig. 9 for all eight radial functions.

B. Screening

In evaluating the screening effect, we again exploit the fact that we are really only interested in the wave functions at the nucleus, their behavior elsewhere in the atom being of consequence only insofar as it affects the normalization. At the nucleus or near it, the potential felt by an electron is essentially unscreened—the nuclear charge is near and therefore acting strongly, while the other electrons are far away. As a result, the wave functions in the nuclear region have the same functional form as for a "hydrogen-like" atom, but with an altered normalization factor. The ratio ρ of the two Dirac radial functions obeys an inhomogeneous nonlinear equation and, as stated before, no normalization problem arises for it; since the potential is essentially unscreened in the nuclear region, ρ is the same as without screening, i.e., screening affects the two functions in the same manner. We can thus define for every shell or subshell a screening factor, as the change in normalization. The SEAC computation of the K and L internal conversion coefficients[14] includes values for the normalization of the bound state K and L wave functions for a Coulomb potential modified for screening effects. Since the functional form is the analytically known one for the

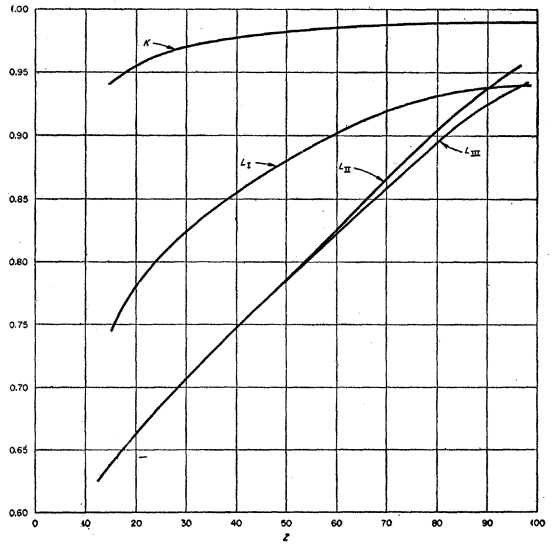

FIG. 10. Ratio of the radial wave functions at the nuclear radius for a screened atom to the corresponding wave functions in a pure Coulomb field. This ratio applies to both large and small wave functions.

Coulomb field, we have the wave functions at small r for a screened field. We have independently computed the wave functions for a Coulomb field with finite-size corrections added. For the "large component" radial function (which is relatively insensitive to the finite-size correction), we multiply the finite-size wave function by the screening factor. For the other radial function, this result is multiplied by the ratio ρ of wave functions computed with the correct eigenvalues (including both finite-size and screening). This last refinement is not very important, as the results are rather insensitive to the exact energy value because the potential greatly exceeds the binding energy in the nuclear region. For the K shell and the L_{I} subshell, we had a rough check in Reitz' tables of screened wave functions[18] (the accuracy of this check was limited by difficulty of interpolation in these tables). The screening factors are given in Fig. 10.

C. Average over the Nuclear Volume

The transition probability involves an integral over the nuclear volume whose absolute value squared is summed over magnetic quantum numbers. In terms of any coupling scheme, the angular integration and the summation can be carried out, yielding the usual Clebsch-Gordan and Racah coefficients expressing the angular momentum and parity selection rules. There remains a radial integral

$$\int_0^R r^2 dr \Re_f^* T_\Omega(r) \Re_i L(r), \tag{8}$$

[18] J. R. Reitz, *Relativistic Electron Wave Functions for a Fermi-Thomas-Dirac Statistical Atom* (University of Chicago Press, Chicago, Illinois, 1949).

where the $\mathfrak{R}$ are the nuclear radial functions, T_Ω is a radial operator whose form depends on the choice of interaction Ω, and $L(r)$ is a bilinear combination of the electron and neutrino radial functions. This integral combines the rather accurately known lepton functions with the poorly known nuclear functions. The neutrino radial functions are spherical Bessel functions[19] which for small r (in the nucleus) are quite accurately

$$f_{\kappa'}{}' \sim r^{l'(-\kappa')}, \quad g_{\kappa'}{}' \sim r^{l'(\kappa')}, \tag{9}$$

where l' is the "orbital angular momentum" corresponding to the κ value given by the subscript. For the electron functions, we go back to the inside solution of the finite-size nucleus. The quadrature solution of the two coupled Dirac radial equations[15] immediately supplies us with the indicial behavior of the radial functions,

$$f_\kappa \sim r^{l(-\kappa)}, \quad g_\kappa \sim r^{l(\kappa)}, \tag{10}$$

and yields an infinite series whose terms differ by an even integral power of r, oscillate in sign, and decrease in magnitude; the convergence and sign alternation are preserved if the series is reordered into a power series. Knowing these properties, the solution for a particular potential is achieved by substituting the two functions, expressed as the indicial factor times a power series in r^2, into the coupled radial equations, thus obtaining recursion relations between the coefficients.[3] It turns out in our case that four terms in the series give an accuracy of better than 0.1% even for the highest Z. We can now perform some sort of average on the power series, leaving an integral

$$\int_0^R r^2 dr \mathfrak{R}_f{}^* T_\Omega \mathfrak{R}_i r^{l+l'}, \tag{11}$$

which is independent of lepton characteristics (except for the trivial appearance of the orbital angular momenta which merely reflect the selection rules). This matrix element is the same for capture of any orbital electron, and for beta decay for that matter. The traditional procedure[7] amounts to evaluating the series at the nuclear surface. Instead, we have used a uniform weighting over the nuclear volume. For the large components, the two procedures differ by only five percent at most. For the small components, the discrepancy is larger, but then the small components only occur where there is a mixture of matrix elements, so that there is merely added a small uncertainty to a much larger one. In short, for a nucleus of finite-size, the variation of the wave functions over the nuclear volume is so small that the method of averaging matters little.

[19] M. E. Rose and R. K. Osborn, Phys. Rev. **93**, 1315 (1954).

Erratum: Normal Modes of Aluminum by Neutron Spectrometry

[Revs. Modern Phys. **30**, 236 (1958)]

B. N. Brockhouse and A. T. Stewart
Physics Division, Atomic Energy of Canada, Ltd., Chalk River, Ontario, Canada

In the legend of Fig. 13 the filled circles for [110] directions should have $\alpha=(0,0,1)$ and the filled squares $\alpha=1/\sqrt{2}(1,\bar{1},0)$.